Figure Legends

Figure 1. Dnmt3b expression in murine and human knee joint cartilage. (A) Representative images showing that Dnmt3a is not expressed in chondrocytes from 3 mo WT articular cartilage [Dnmt3a expression in pancreas tissue (positive control)], while robust expression of Dnmt3b in chondrocytes of 3 mo WT articular cartilage and lower expression in underlying growth plate cartilage (n=3); the magnified images of the dashed and solid boxed area of articular cartilage in separate panels; (B) Representative images showing Dnmt3b expression in 3 mo (n=3) versus 27 mo (n=3) WT murine knee articular cartilage; (C) Representative images showing Dnmt3b expression in 14 wk old murine articular cartilage following MLI surgery (n=3) or cartilage from sham control knees (n=3); (D) Representative images showing Dnmt3b expression in 14 wk old murine articular cartilage in mice fed a high fat diet (HFD) (n=3) or controls (Ctrl) fed a normal diet (n=3). (E) Two representative images showing DNMT3B expression in human healthy articular cartilage (n=11) or osteoarthritic cartilage tissue sections (n=71). (F) Reduced *DNMT3B* expression in human primary OA chondrocytes compared to healthy chondrocytes (n=3). (G) Induction of human primary chondrocytes (n = 3) with IL-1β results in decreased expression of DNMT3B mRNA and protein levels. All scale bars, 100 μm.

Figure S1. Dnmt3b expression in embryonic and adult murine knee joint cartilage. Immunohistochemical staining shows Dnmt3b protein expression in chondrocytes from C57BL/6 WT murine articular cartilage knee joints at embryonic time point E18.5 and post-natal time points P7, P28 and P56 (n=3). *, hypertrophic chondrocyte; **, bone marrow cells. All scale bars, 100 μm.

Figure S2. Altered anabolic and catabolic gene expression in IL-1β-treated human primary chondrocytes. Reduced *COL2A1* and increased *MMP13* expression following IL-1β treatment (48 h) of human primary articular chondrocytes isolated from total knee replacement surgeries (n=3).

Figure S3. IL-1β regulation of Dnmt3b is mediated in part by NF-κB. (A) Sequence alignment and conservation of an NF-κB binding site (red) in the promoter region of the *Dnmt3b* gene of different

species. (B) Reduced luciferase expression in IL-1β stimulated (24 h) chondrogenic murine ATDC-5 cells transfected with a luciferase reporter plasmid containing the *Dnmt3b* promoter sequence when compared to control (Ctrl) untreated cells. Reduced luciferase activity is attenuated when ATDC-5 cells were transfected with a reporter plasmid containing a mutated NF-κB binding site (ATCTGGCTCC) (n=3). (C, D) Pull-down of genomic DNA with an NF-κB antibody (ChIP assay) shows interaction of NF-κB with its binding site in the Dnmt3b promoter region by qPCR (C) and semi-quantitative gel electrophoresis (D) utilizing specific primers to amplify the Dnmt3b promoter region containing the NF-κB binding site (n=3). (E, F) Dnmt3b mRNA and protein levels were reduced in murine WT primary articular chondrocytes (extracted from 3 mo murine knee joints) following IL-1β induction (48 h) (n=3).

Figure S4. Ablation of Dnmt3b in articular chondrocytes in vitro alters cell homeostasis. Reduced expression of (A) *Dnmt3b* mRNA and (B) Dnmt3b protein following transfection with 20nM *Dnmt3b* siRNA for 48 h in murine primary chondrocytes isolated from 3 mo WT mice (n=3). (C) *Dnmt3b* siRNA treatment resulted in increased expression of the catabolic/hypertrophic chondrocyte markers *Col10a1*, *Runx2*, and *Mmp13*, and decreased expression of the anabolic marker, *Col2a1* in murine primary chondrocytes (n=3). (D) Representative images showing reduced Dnmt3b expression resulted in increased alkaline phosphatase (ALP) activity in murine primary chondrocytes, but not to the extent resulting from BMP-2 treatment (positive control) (n=3). (E, F) *Dnmt3b* siRNA treatment affected the balance of TGF-β and BMP signaling as shown by decreased phospho(p)-Smad2 expression and increased p-Smad1/5 expression in murine primary chondrocytes, respectively (n=3).

Figure 2. *Dnmt3b* loss-of-function mice develop accelerated OA. (A) Representative alcian blue / hematoxylin / orange G (ABH/OG) staining of tissue sections of knee joints harvested from 5 mo and 8 mo *Dnmt3b* loss-of-function (LOF) mice and Cre + control (Ctrl) mice (n=5). The magnified images of the boxed regions are shown respectively. (B) OARSI scoring system was used to quantify the ABH/OG stained tissue sections (n=5). (C) Articular cartilage area was quantified by histomorphometry (n=5). (D)

Representative microCT images of knee joints from 8 mo *Dnmt3b* LOF and Ctrl mice (n=5). (E) Subchondral bone volume and (F) subchondral bone trabecular connective density were calculated from the microCT images (n=5). Arrows in 5 mo old *Dnmt3b* LOF mice show areas of proteoglycan loss and cartilage fibrillation, respectively. Arrows in 8 mo old *Dnmt3b* LOF mice show osteophyte formation and an area of proteoglycan loss in articular cartilage, respectively. Yellow arrows in microCT images denote osteophyte formation. Scale bars, 100 μm.

Figure S5. Ablation of Dnmt3b in articular chondrocytes in vivo. (A) Representative fluorescence microscopy shows recombination efficiency in 2 mo *Agc1Cre^{ERT2}; mT/mG* mice followed by tamoxifen injection for 5 days (n=3). (B) Dnmt3b protein knock-down in 3 mo articular chondrocytes of *Dnmt3b* LOF mice compared to Cre + control (Ctrl) littermates (n=3). Scale bars, 100 μm.

Figure S6. Expression of *Dnmt* as well as anabolic and catabolic genes in *Dnmt3b* LOF cartilage tissue. (A) qPCR analysis of *Dnmts* and *Tets* in 3 mo articular cartilage isolated from *Dnmt3b* LOF and Cre+ control (Ctrl) mice (n=3). (B) Tet activity analysis in chondrocytes from 3 mo *Dnmt3b* LOF or Ctrl mice (n=3). (C)*Col2a1* (anabolic) and *Col10a1*, *Runx2* and *Mmp13* (catabolic / hypertrophic) marker expression in articular chondrocytes from 3 mo *Dnmt3b* LOF and Cre + control (Ctrl) mice (n=3).

Figure S7. Analysis of apoptosis and reactive oxygen species in *Dnmt3b* LOF cartilage. (A) Representative TUNEL staining and analysis of knee joint articular cartilage tissue sections from 5 mo *Dnmt3b* LOF and Cre+ control (Ctrl) mice by fluorescence microscopy (n=5); (B) Quantification of apoptotic cell numbers from the TUNEL-stained fluorescent images (n=5). (C) Reactive oxygen species (ROS) analysis of 2 mo *Dnmt3b* LOF articular chondrocytes (i.e. chondrocytes from *Dnmt3b$^{f/f}$* mice treated with Ad5-Cre for 48 h) compared to control (Ctrl) chondrocytes (*Dnmt3b* LOF chondrocytes treated with Ad5-GFP for 48 h) (n=3).

Figure 3. Altered epigenomic and transcriptomic signatures in *Dnmt3b* LOF chondrocytes. gDNA and RNA isolated from control and Dnmt3b LOF cells for RNA-seq and methylC-seq analysis (n=3). (A)

PCA plot of samples based on RNA-seq data; (B) Heatmap display of top 25 significantly differentially expressed genes between *Dnmt3b* LOF and control; (C) Word cloud representing gene frequency of enriched function categories from all differentially expressed genes; (D) Global methylation distribution of *Dnmt3b* LOF and control samples showing there is no global difference; (E) Methylation difference of DMR versus genome as background; (F) Significant overlap of genes nearby DMRs and differentially expressed genes, p-values calculated by hypergeometric test.

Figure S8. Analysis of RNA-seq and methylC-seq data. (A) Heatmap of sample-to-sample distances using the rlog-transformed values showing more similarity of RNA-seq signal observed in each group; (B) An MA-plot of gene expression changes. The log2 fold change for a particular comparison is plotted on the y-axis and the average of the counts normalized by size factor is shown on the x-axis. Each gene is represented with a dot. Genes with an adjusted p value below a threshold (here 0.1, the default) are shown in red; (C) Enrichment of differentially expressed genes show enriched function related to cell cycle process, bone development etc; (D) Genes from differentially expressed list are related with TGF/BMP pathway network, green indicates down-regulation and red indicates up-regulation; (E) Genomic feature distributions of DMRs; (F) Enriched transcription factor binding sites found in DMRs using Homer software. n=3.

Figure 4. Mitochondria function and cellular homeostasis in *Dnmt3b* LOF chondrocytes. Primary articular chondrocytes were isolated from 2 mo *Dnmt3b*$^{f/f}$ mice and infected with Ad5-Cre (*Dnmt3b* LOF) or Ad5-GFP (Ctrl) for 48 h. (A) Mitochondrial respiration was measured by the Seahorse XF Extracellular Flux Analyzer. Basal respiration and maximal respiration, as measured by the oxygen consumption rate (OCR) are shown (n=8). (B) TCA metabolite (succinate, fumarate) and NADH analysis by HPLC-MS (n=3). (C) Mitochondrial metabolism analysis was measured in 2 mo WT cells treated with either 1mM diethyl succinate or vehicle for 48 h by the Seahorse XF Extracellular Flux Analyzer (n=8). (D) Mitochondrial respiration analysis in BMP-2-treated 2 mo WT chondrocytes in the presence or absence antimycin A + rotenone for 48 h (n=8).

Figure S9. Chondrocyte gene expression in *Dnmt3b* LOF cells. Primary articular chondrocytes were isolated from 2 mo *Dnmt3b*$^{f/f}$ mice and infected with Ad5-Cre (*Dnmt3b* LOF) or Ad5-GFP (Ctrl) for 48 h. Expression of anabolic (*Col2a1*) or catabolic/hypertrophic genes (*Col10a1*, *Runx2*, *Mmp13*) is shown (n=3).

Figure S10. Chondrocyte gene expression under succinate treatment. Primary articular chondrocytes from 2 mo WT mice were treated with 1mM diethyl succinate or vehicle for 48 h. (A) Cellular succinate levels in murine chondrocytes (n=3). (B) Chondrocyte gene expression in response to succinate treatment was analyzed by qPCR (n=3).

Figure S11. Chondrocyte gene expression under antimycin A and rotenone (A&R) treatment. Primary articular chondrocytes form 2 mo WT mice were treated with 0.1 μM antimycin A and rotenone for 48 h. (A) Effect of antimycin A and rotenone treatment on chondrocyte proliferation and apoptosis (n=3). (B) Analysis of chondrocyte gene expression in response to BMP-2 treatment + / - antimycin A + rotenone (n=3).

Figure 5. *Dnmt3b* gain-of-function mice are protected from cartilage degeneration following surgical induction of OA. MLI or sham surgeries were performed on *Dnmt3b* gain-of-function (GOF) mice or Cre + control (Ctrl) mice. (A) Alcian blue / hematoxylin / orange G stained sections of Ctrl or *Dnmt3b* GOF knee joints 12 weeks following sham surgery. Representative images of histological sections from Ctrl or *Dnmt3b* GOF mice at 8 wk or 12 wk following MLI surgery (n=5). The magnified images of the boxed regions are shown respectively. (B) Quantitation of histological assessment by OARSI scoring (n=5). (C) Histomorphometric analysis of Ctrl or *Dnmt3b* GOF cartilage (n=5). Scale bars, 100 μm.

Figure 6. Mitochondria function and cellular homeostasis in *Dnmt3b* GOF chondrocytes. (A) Gene expression in chondrocytes isolated from 10 wk Ctrl or *Dnmt3b* GOF chondrocytes (n=3). (B) Mitochondrial respiration in primary articular chondrocytes isolated from 2 mo *Col2a1Cre; Rosa-rtTA*$^{f/+}$*;*

Dnmt3b-tg mice, treated with vehicle (Ctrl) or doxycycline (*Dnmt3b* GOF) for 48 h (n=3). Mitochondrial respiration was measured by the Seahorse XF Extracellular Flux Analyzer.

Figure S12. Generation of *Dnmt3b gain-of-function* (GOF) transgenic mice. (A) Schematic representation of the strategy utilized to generate doxycycline (DOX)-inducible *Dnmt3b* over-expression in murine cartilage tissue. (B) Genotyping strategy, utilizing three different primer pairs, to confirm recombination. Mouse line #9 was used for breeding and subsequent experimental analyses.

Figure S13. Over-expression of *Dnmt3b* in articular chondrocytes in vivo. (A) Representative fluorescence microscopy shows recombination efficiency in 10 wk *Col2a1Cre; Rosa-rtTA$^{f/+}$; H2BGFP* mice (n=3). Scale bar, 100 μm. (B) Confirmation of Dnmt3b protein over-expression in primary articular chondrocytes from 10 wk *Dnmt3b* GOF or Cre + control (Ctrl) mice by Western blotting using Dnmt3b antibodies (n=3).

Figure S1

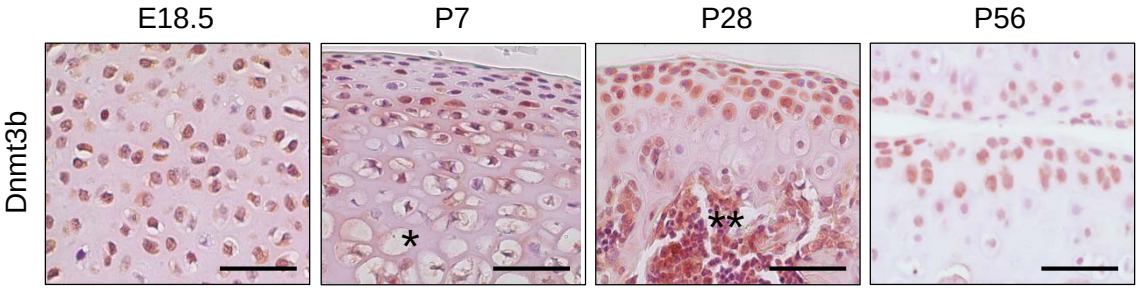

Figure S2

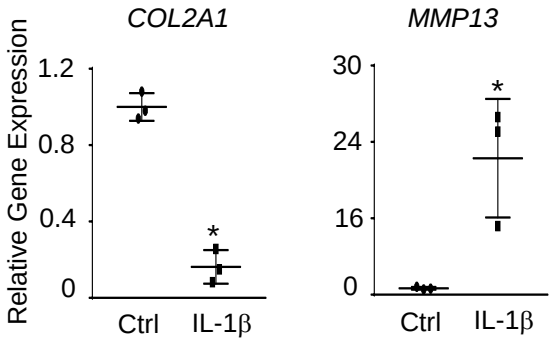
COL2A1
MMP13
Relative Gene Expression
1.2
0.8
0.4
0
30
24
16
0
*
*
Ctrl
IL-1β
Ctrl
IL-1β

Figure S3

A

Mouse	-182	GGGGGCCCAGGGGAGGCTCCCGAGGAGGCA -153
Human	-169	AGGGGCGGAGGGGAGGCTCCGAGCGATTTC -140
Dog	-386	CAAGGCTGTCGGGAGGCAGGCAGGGGCAGG -357
Horse	-90	AGGCATTGGCGGGAGGTTTGGGGATGTGCT -61

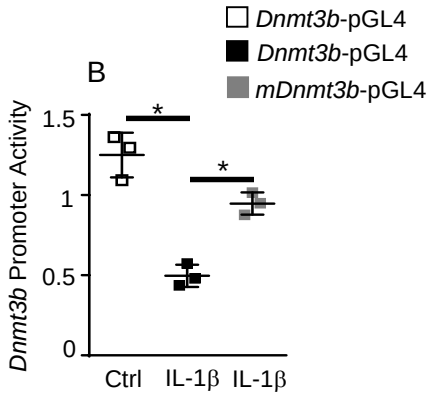

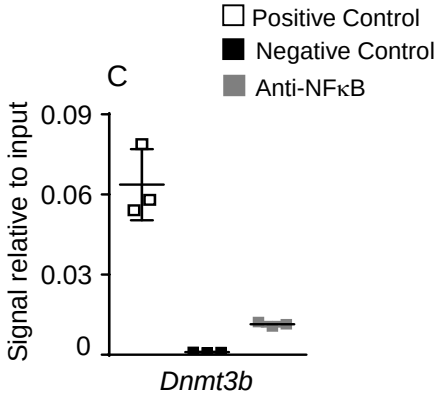

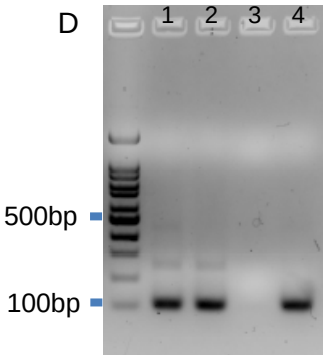

1: Input
2: Positive control
3: Negative control
4: Anti-NFκB

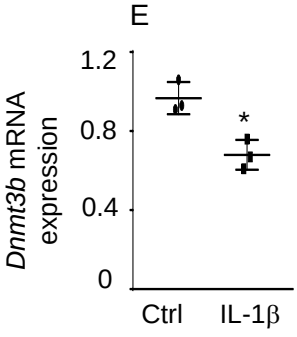

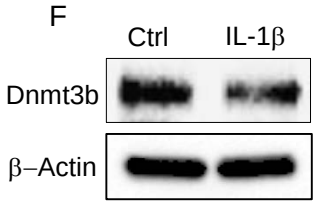

Figure S4

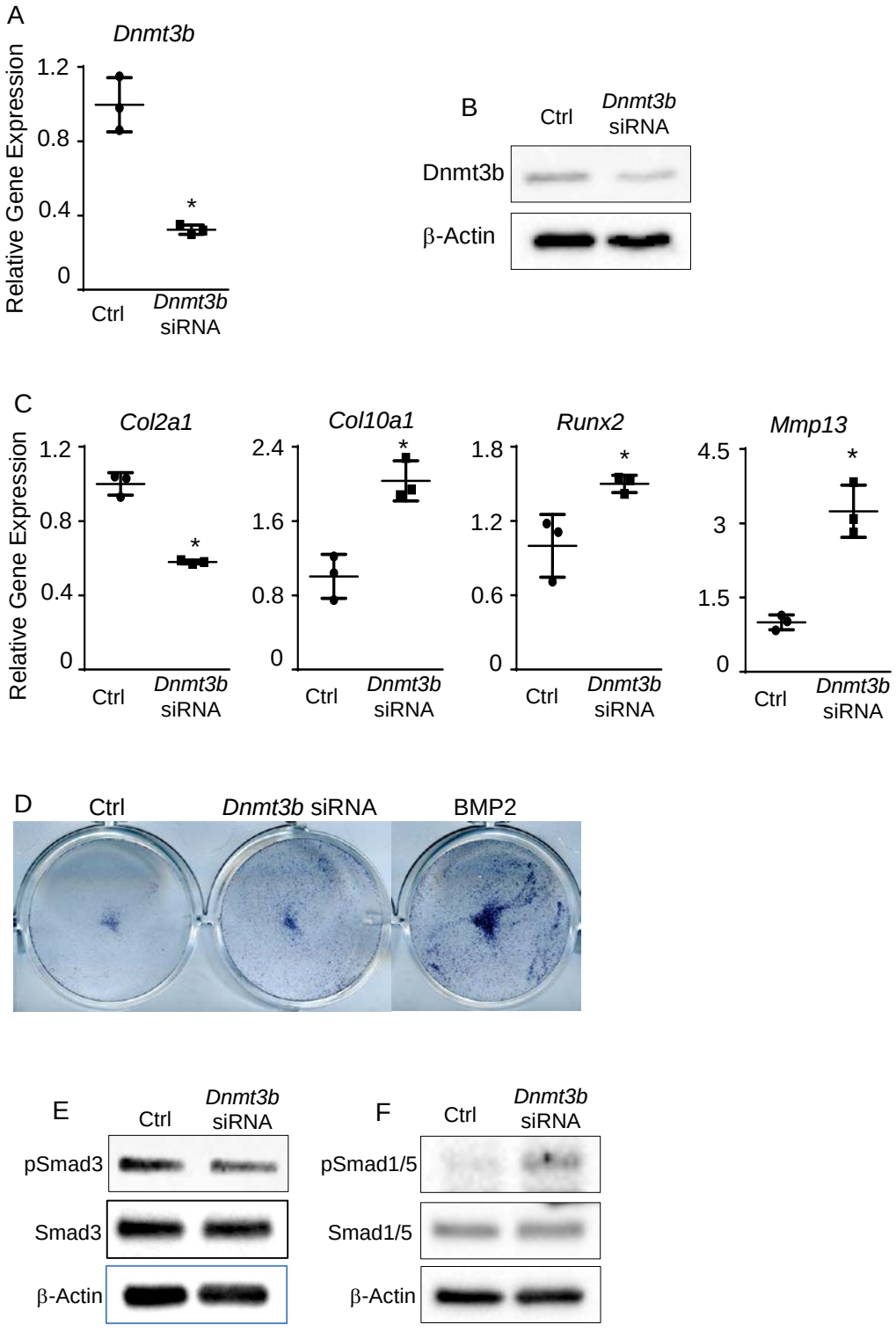
A
Dnmt3b
Relative Gene Expression
1.2
0.8
0.4
0
*
Ctrl
Dnmt3b siRNA
B
Ctrl
Dnmt3b siRNA
Dnmt3b
β-Actin
C
Col2a1
Col10a1
Runx2
Mmp13
Relative Gene Expression
2.4
1.6
1.8
1.2
0.6
4.5
3
1.5
Ctrl
Dnmt3b siRNA
D
Ctrl
Dnmt3b siRNA
BMP2
E
Ctrl
Dnmt3b siRNA
pSmad3
Smad3
β-Actin
F
Ctrl
Dnmt3b siRNA
pSmad1/5
Smad1/5
β-Actin

Figure S5

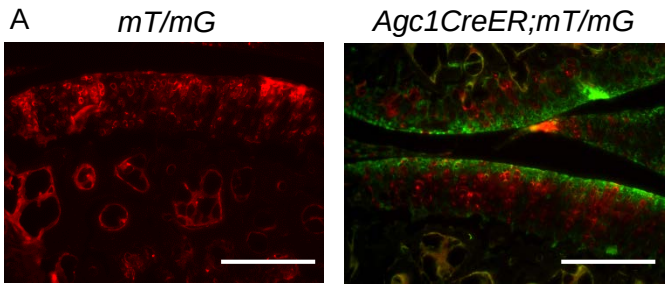

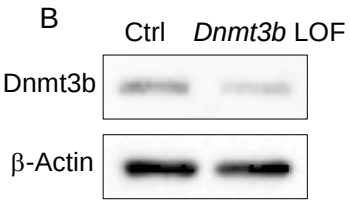

Figure S6

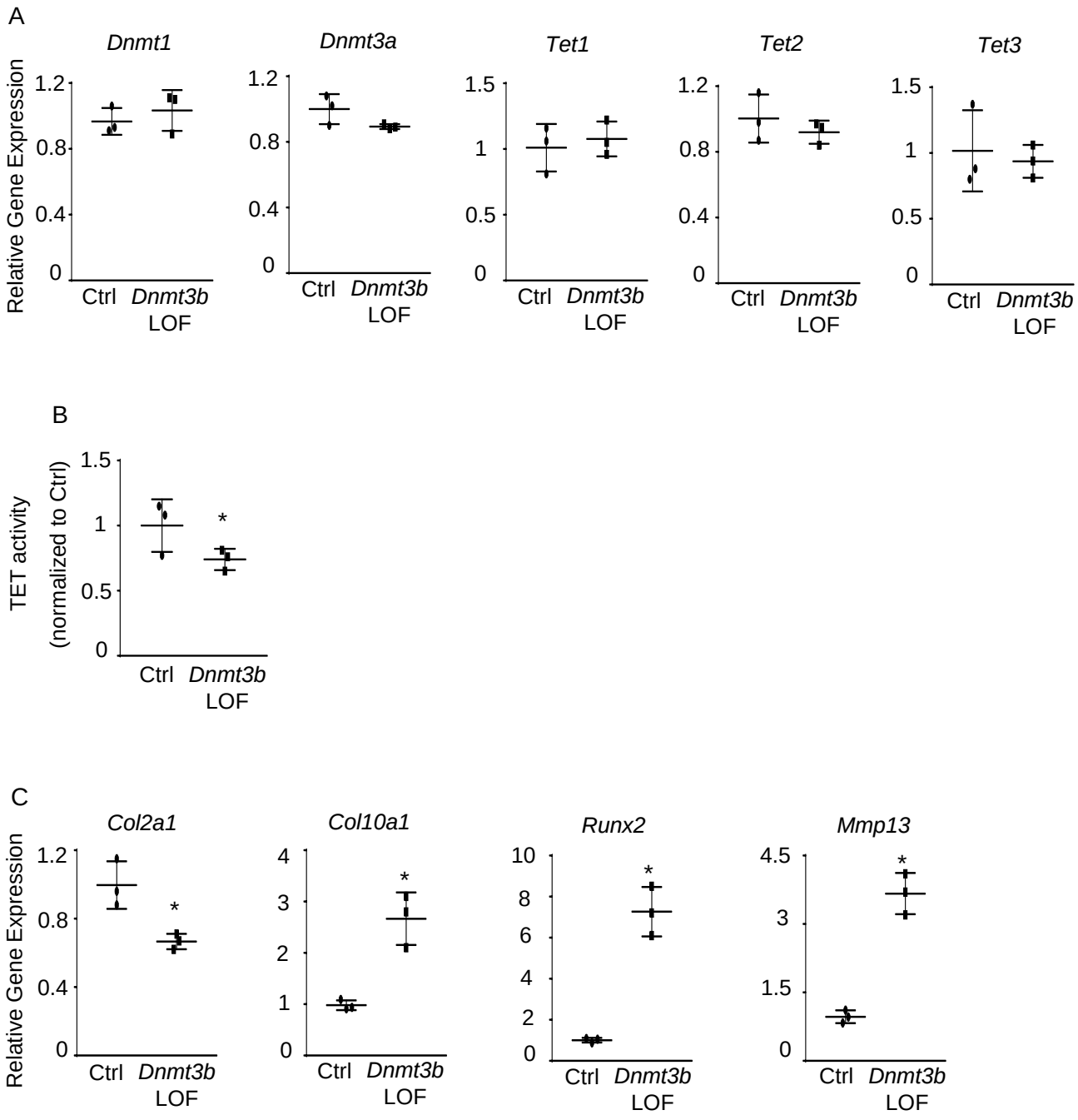
A
Dnmt1
Dnmt3a
Tet1
Tet2
Tet3
Relative Gene Expression
Ctrl
Dnmt3b LOF
B
TET activity (normalized to Ctrl)
*
C
Col2a1
Col10a1
Runx2
Mmp13

Figure S7

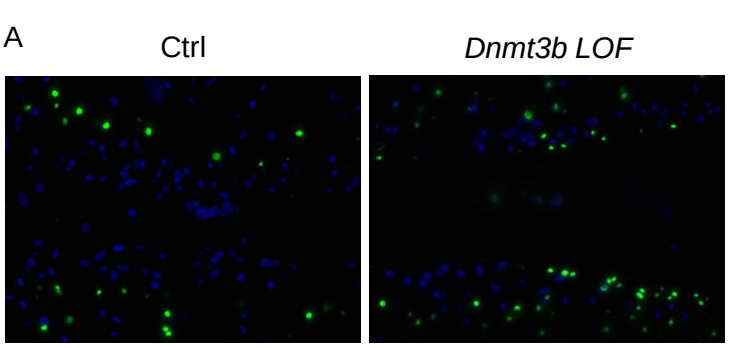
A
Ctrl
Dnmt3b LOF

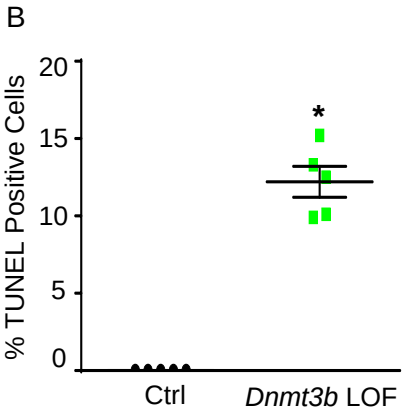
B
% TUNEL Positive Cells
20
15
10
5
0
*
Ctrl
Dnmt3b LOF

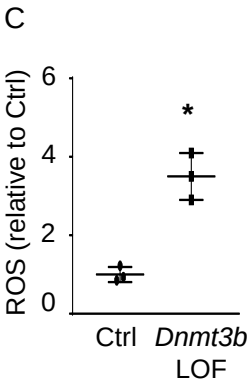
C
ROS (relative to Ctrl)
6
4
2
0
*
Ctrl
Dnmt3b
LOF

Fig. S8

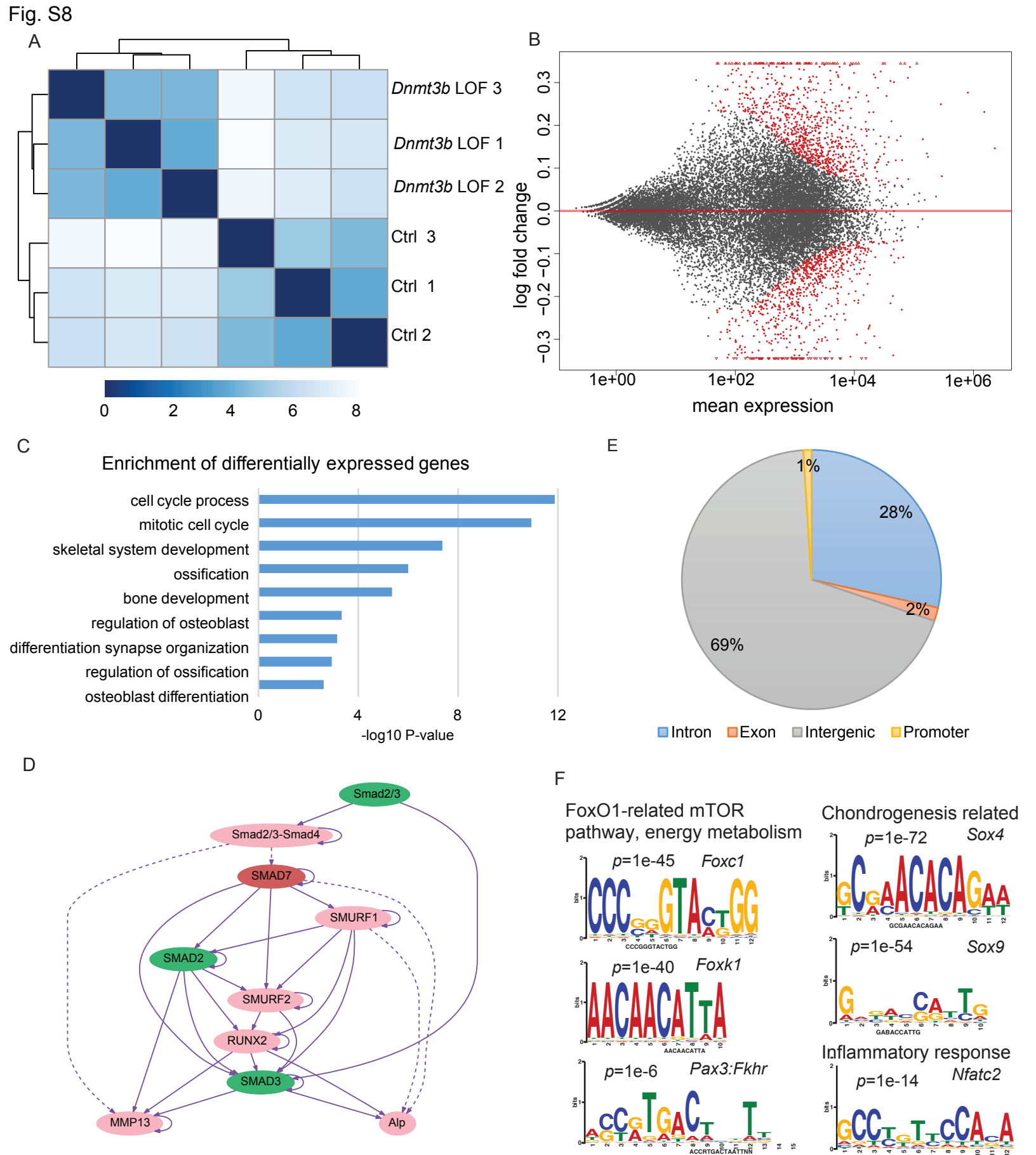
A
Dnmt3b LOF 3
Dnmt3b LOF 1
Dnmt3b LOF 2
Ctrl 3
Ctrl 1
Ctrl 2
0
2
4
6
8
B
log fold change
0.3
0.2
0.1
0.0
−0.1
−0.2
−0.3
1e+00
1e+02
1e+04
1e+06
mean expression
C
Enrichment of differentially expressed genes
cell cycle process
mitotic cell cycle
skeletal system development
ossification
bone development
regulation of osteoblast
differentiation synapse organization
regulation of ossification
osteoblast differentiation
0
4
8
12
-log10 P-value
D
Smad2/3
Smad2/3-Smad4
SMAD7
SMURF1
SMAD2
SMURF2
RUNX2
SMAD3
MMP13
Alp
E
1%
28%
2%
69%
Intron
Exon
Intergenic
Promoter
F
FoxO1-related mTOR pathway, energy metabolism
p=1e-45
Foxc1
CCCGGGTACTGG
p=1e-40
Foxk1
AACAACATTA
p=1e-6
Pax3:Fkhr
ACCRTGACTAATTNN
Chondrogenesis related
p=1e-72
Sox4
GCGAACACAGAA
p=1e-54
Sox9
GABACCATTG
Inflammatory response
p=1e-14
Nfatc2

Figure S9

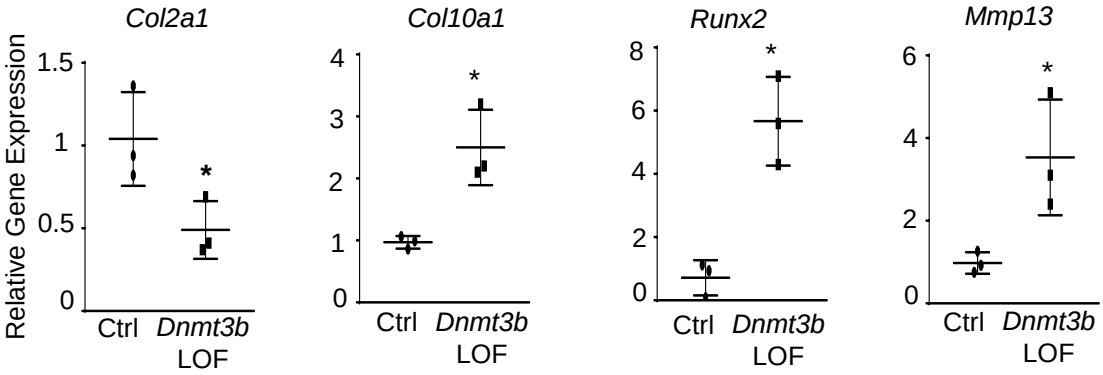
Col2a1
Col10a1
Runx2
Mmp13
Relative Gene Expression
1.5
1
0.5
0
4
3
2
1
0
8
6
4
2
0
6
4
2
0
*
Ctrl
Dnmt3b
LOF

Figure S10

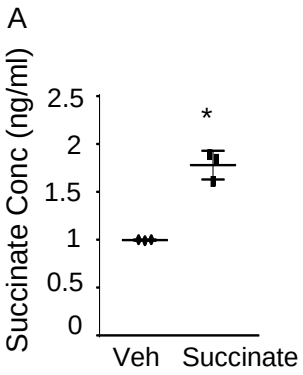
A
Succinate Conc (ng/ml)
2.5
2
1.5
1
0.5
0
*
Veh
Succinate

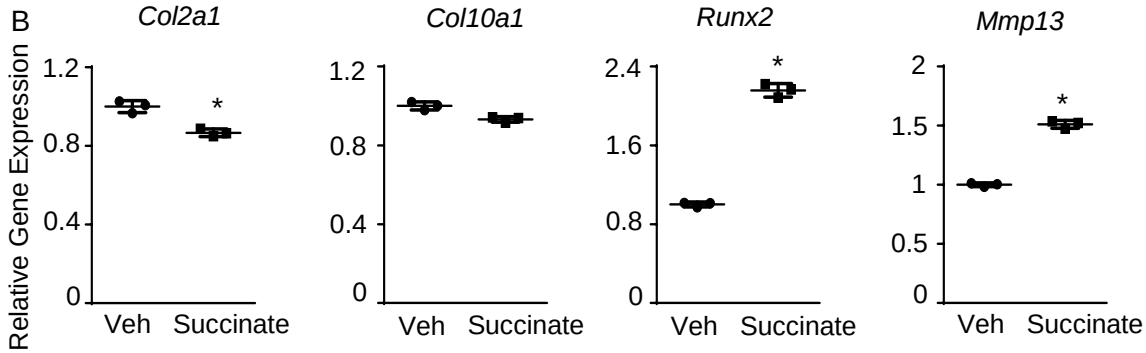
B
Relative Gene Expression
Col2a1
1.2
0.8
0.4
0
*
Veh
Succinate
Col10a1
1.2
0.8
0.4
0
Veh
Succinate
Runx2
2.4
1.6
0.8
0
*
Veh
Succinate
Mmp13
2
1.5
1
0.5
0
*
Veh
Succinate

Figure S11

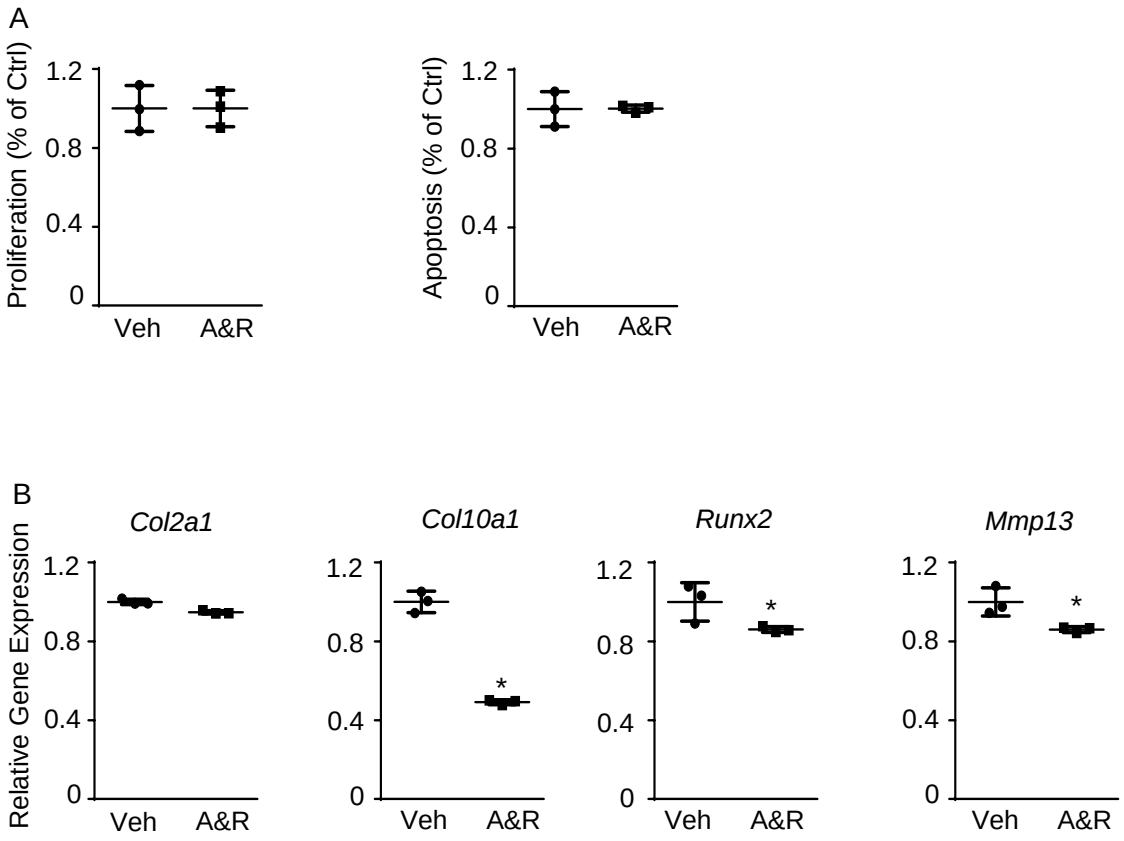
A
Proliferation (% of Ctrl)
1.2
0.8
0.4
0
Veh
A&R
Apoptosis (% of Ctrl)
1.2
0.8
0.4
0
Veh
A&R
B
Relative Gene Expression
Col2a1
Col10a1
Runx2
Mmp13
1.2
0.8
0.4
0
*
Veh
A&R

Figure S12

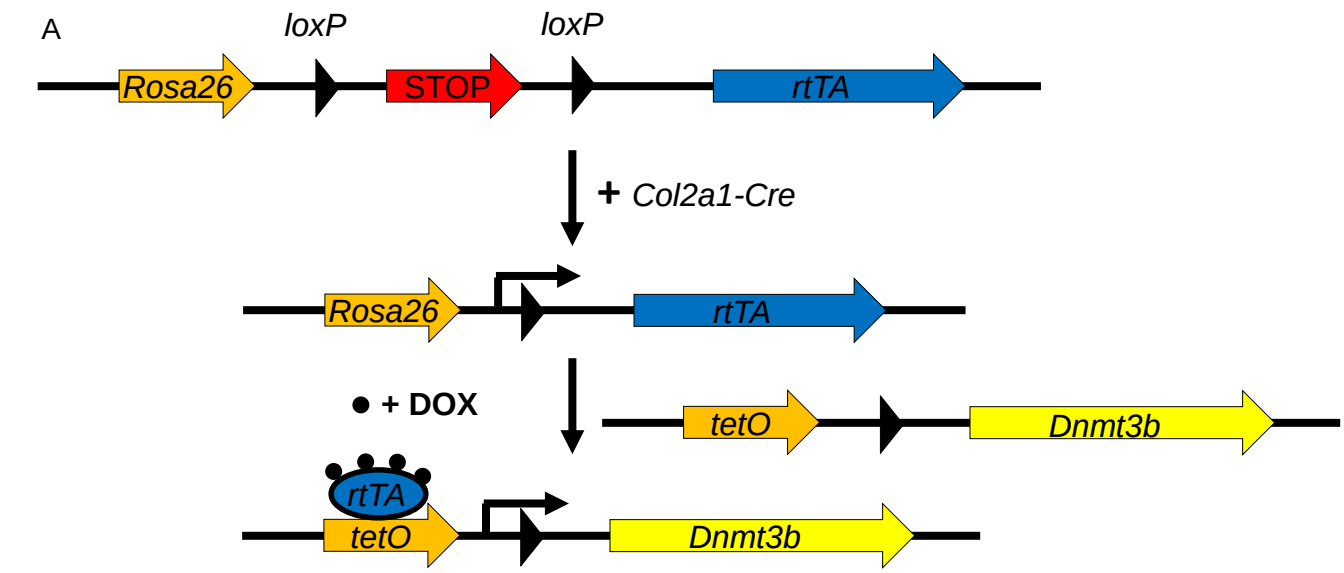
A
loxP
loxP
Rosa26
STOP
rtTA
+ Col2a1-Cre
Rosa26
rtTA
● + DOX
tetO
Dnmt3b
rtTA
tetO
Dnmt3b

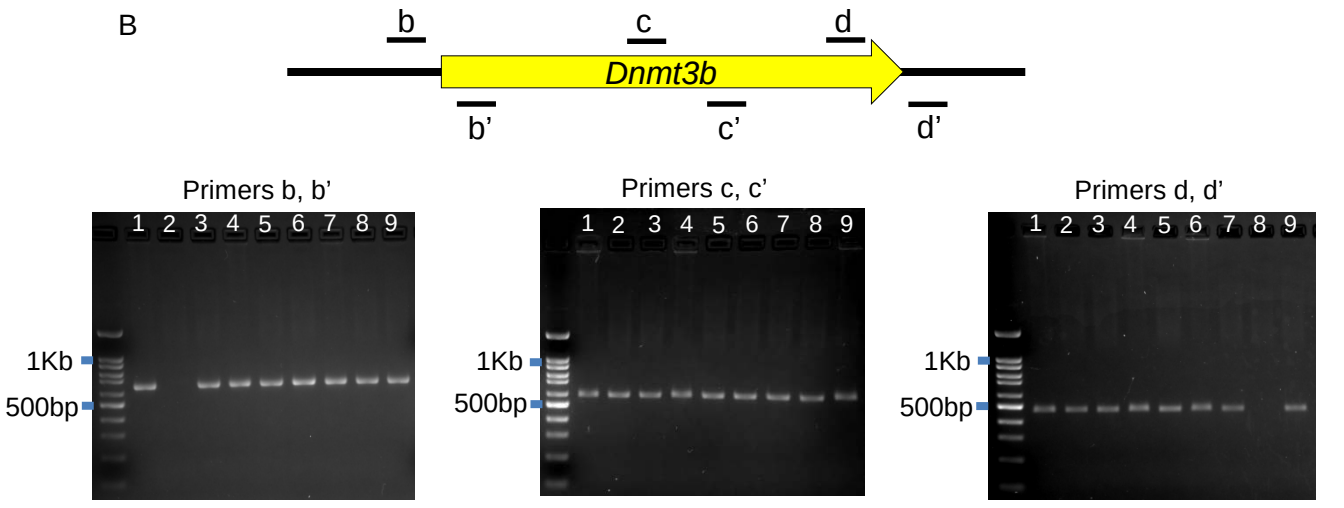
B
b
c
d
Dnmt3b
b'
c'
d'
Primers b, b'
1 2 3 4 5 6 7 8 9
1Kb
500bp
Primers c, c'
1 2 3 4 5 6 7 8 9
1Kb
500bp
Primers d, d'
1 2 3 4 5 6 7 8 9
1Kb
500bp

Figure S13

A *Col2Cre;Rosa-rtTA$^{f/+}$;H2BGFP*

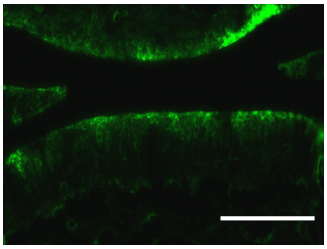

B